Anal. Chem. **2006,** *78,* 6792−6800

Exploring Crown Ethers as Shift Reagents for Ion Mobility Spectrometry

Amy E. Hilderbrand, Sunnie Myung, and David E. Clemmer*

Department of Chemistry, Indiana University, Bloomington, Indiana 47405

A series of crown ethers, 12-crown-4, 15-crown-5, 18-crown-6, and dibenzo-30-crown-10, are examined as a possible means of shifting the mobilities of peptide ions. In this approach, a crown ether is added to a solution containing a mixture of peptides and is electrosprayed into the gas phase in order to create distributions of peptide−crown complexes. The ion complexes have different mobilities than the naked peptide ions, and the crown ether molecules appear to interact specifically with basic sites in the peptides thus providing some sequence selectivity. After the peptide−crown complexes are separated by ion mobility spectrometry, the ions can be collisionally activated to dissociate the complex (forming the naked peptide ions) prior to *m/z* analysis. The overall effect is that complex formation shifts peptide ions to different regions of the mobility spectrum, extending the ability to resolve components. The approach is illustrated by examining isobaric dipeptides as well as a combinatorial library containing 27 tripeptides. Cross sections for the series of crown ether ions and complexes that are observed are reported.

During the past decade there has been considerable interest in using ion mobility spectrometry (IMS) as an analytical approach for the analysis of complex biological mixtures.[1−6] The added dimension of separation associated with IMS complements other techniques, such as liquid chromatography and mass spectrometry (MS), increasing the peak capacity and information content associated with complex samples.[1,3,4,6−8] Although these techniques are proving useful, an inherent limitation arises when IMS is coupled with MS. In IMS, ions are separated based on their size and charge state, and size is correlated with mass, limiting the effective peak capacity of the IMS−MS combination. For example, consider the variation in mobilities associated with a narrow mass range of $[M + H]^+$ peptides (e.g., 700−710 Da). Typically, the range of mobilities at these ions is less than ∼20%.[9,10] For IMS resolving powers ($R = t_D/\Delta t_D$, where t_D is the drift time and Δt_D is the full width at half-maximum of the peak) of 20−100, the maximum increase in peak capacity (for this single charge state and narrow m/z range) is only a factor of 5−20 times the value obtained from MS alone. For this reason, there is a need to develop techniques that bypass the intrinsic correlation of size and mass.

To do this, it is instructive to consider the mechanism of separation in more detail. Ion mobility separations are governed by a momentum transfer process between an ion and a buffer gas.[11−13] Although there have been several attempts to shift peak positions by using different buffer gases, ultimately there is little difference in the relative interactions of different gases within a given distribution of ions.[14−17] This is largely because changes associated with the long-range nature of ion-induced dipole interactions imposed by a different gas lead to relatively similar shifts in the mobilities for ions with similar chemical and physical

* To whom correspondence should be addressed. E-mail: clemmer@indiana.edu.

(1) Henderson, S. C.; Valentine, S. J.; Counterman, A. E.; Clemmer, D. E. *Anal. Chem.* **1999**, *71*, 291−301.
(2) Valentine, S. J.; Counterman, A. E.; Hoaglund, C. S.; Reilly, J. P.; Clemmer, D. E. *J. Am. Soc. Mass Spectrom.* **1998**, *9*, 1213−1216.
(3) Valentine, S. J.; Kulchania, M.; Srebalus Barnes, C. A.; Clemmer, D. E. *Int. J. Mass Spectrom.* **2001**, *212*, 97−109.
(4) Gillig, K. L.; Ruotolo, B.; Stone, E. G.; Russell, D. H. Fuhrer, K.; Gonin, M.; Schultz, A. J. *Anal. Chem.* **2000**, 72, 3965−3971.
(5) Wu, C.; Siems, W. F.; Klasmeier, J.; Hill, H. H., Jr. *Anal. Chem.* **2000**, 72, 391.
(6) Guevremont, R.; Barnett, D. A.; Purves, R. W.; Vandermey, J. *Anal. Chem.* **2000**, *72*, 4577−4584. Barnett, D. A.; Ells, B.; Guevremont, R.; Purves R. W. *J. Am. Soc. Mass Spectrom.* **2002**, *13*, 1282−1291.
(7) Venne, K.; Bonneil, E.; Eng, K.; Thibault, P. *Anal. Chem.* **2005**, 77, 2176−2186.
(8) Li, J. J.; Purves, R. W.; Richards, J. C. *Anal. Chem.* **2004**, 4676−4683.
(9) See for example, data from: Srebalus, C. A.; Li, J.; Marshall, W. S.; Clemmer, D. E. *Anal. Chem.* **1999**, *71*, 3918−3927. Srebalus, C. A.; Li, J.; Marshall, W. S.; Clemmer, D. E. *J. Am. Soc. Mass Spectrom.* **2000**, *11*, 352−355.
(10) We note that the range of mobilities increases with increasing peptide length; protein cross sections (within a specific charge state) may vary by more than 100%. See, for examples: Covey, T.; Douglas, D. J. *J. Am. Soc. Mass Spectrom.* **1993**, *4*, 616−623. Clemmer, D. E.; Hudgins, R. R.; Jarrold, M. F. *J. Am. Chem. Soc.* **1995**, *117*, 10141−10142. Shelimov, K. B.; Clemmer, D. E. Hudgins, R. R.; Jarrold, M. F. *J. Am. Chem. Soc.* **1997**, *119*, 2240−2248. Valentine, S. J.; Counterman, A. E.; Clemmer, D. E. *J. Am. Soc. Mass Spectrom.* **1997**, 8, 954−961. Clemmer, D. E.; Jarrold, M. F. *J. Mass Spectrom.* **1997**, *32*, 577−592. Hoaglund Hyzer, C. S.; Counterman, A. E.; Clemmer, D. E. *Chem. Rev.* **1999**, *99*, 3037−3079. Valentine, S. J.; Counterman, A. E.; Clemmer, D. E. *J. Am. Soc. Mass Spectrom.* **1999**, 10, 1188−1211.
(11) Mason, E. A.; McDaniel, E. W. *Transport Properties of Ion in Gases*; Wiley: New York, 1988.
(12) von Helden, G.; Hsu, M. T.; Kemper, P. R.; Bowers, M. T. *J. Chem. Phys.* **1991**, *93*, 3835−3837. von Helden, G.; Hsu, M. T.; Gotts, N.; Bowers, M. T. *J. Phys. Chem.* **1993**, *97*, 8182−8192.
(13) Shvartsburg, A. A.; Jarrold, M. F. *Chem. Phys. Lett.* **1996**, *261*, 86−91. Mesleh, M. F.; Hunter, J. M.; Shvartsburg, A. A.; Schatz, G. C.; Jarrold, M. F. *J. Phys. Chem.* **1996**, *100*, 16082−16086.
(14) Asbury, G. R.; Hill, H. H. *Anal. Chem.* **2000**, *72*, 580−584.
(15) Beegle, L. W.; Kanik, I.; Matz, L.; Hill, H. H. *Int. J. Mass Spectrom.* **2002**, *216*, 257−268.
(16) Matz, M. L.; Hill, H. H.; Beegle, L. W.; Kanik, I. *J. Am. Soc. Mass Spectrom.* **2002**, *13*, 300−307.
(17) Ruotolo, B. T.; McLean, J. A.; Gillig, K. J.; Russell, D. H. *J. Mass Spectrom.* **2004**, *39*, 361−367.

10.1021/ac060439v CCC: $33.50
Published on Web 08/23/2006

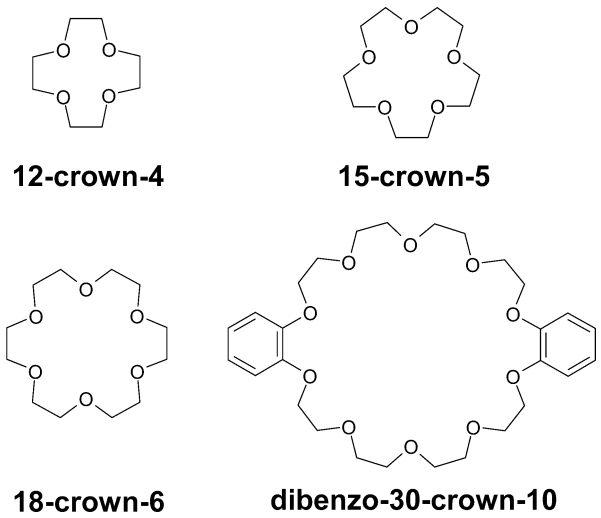

Figure 1. Crown ethers used in these experiments.

properties (e.g., a mixture of peptide ions); therefore, only small changes in the relative mobilities of different ions are observed when different buffer gases are employed. For large ions, such as peptides and proteins, the key parameter for separating similar components with IMS is associated with the ions themselves. The mobility of an ion depends on its shape (and charge state). For ions of the same net charge, mobilities scale inversely with increasing mass. Because of this, it is relatively straightforward to separate mixtures of ions having different masses by IMS; but it is relatively difficult to pull apart species that have similar masses.

In this paper, we investigate the use of ion−molecule complexes of peptide ions with a series of crown ethers as a means of influencing the separation of ions by IMS. Specifically, peptides are electrosprayed from solutions containing one of the crown ethers shown in Figure 1: 12-crown-4 (12C4), 15-crown-5 (15C5), 18-crown-6 (18C6), and dibenzo-30-crown-10 (DB30C10). Crown ethers appear to preferentially form complexes with basic sites within a peptide.[18] The crown ethers complex with peptides by differing amounts, creating complexes that have differing size and charge state, allowing for peptides that initially had similar size and charge state to be separated due to larger differences in the mobility of the complexes. After the ions are separated, it is possible to collisionally activate the complexes and generate the naked peptide ions, which can subsequently be analyzed by MS. The approach is illustrated by examining a mixture of isobaric dipeptides as well as a 27-component tripeptide library.

The present work builds upon a number of studies of the properties of adduct ions.[19−21] Several groups have examined ion−crown complexes in the gas phase.[18,22−25] Additional work has been done involving the ability to select specific chiral forms of a molecule based on the differential formation of molecular adducts.[26−28] Thus, although this is the first use of complex formation as a means of influencing the positions of peaks during IMS separations, this is likely to be a rich and productive area as many fundamental aspects of the chemistry are understood and can be used advantageously.[29−31]

EXPERIMENTAL SECTION

Peptide Synthesis. Peptides were prepared using standard solid-phase fluorenylmethoycarbonyl (Fmoc) peptide chemistry.[32] Three isobaric peptides, RA, KV, and LN, were prepared individually. Synthesis of these dipeptides was trivial and a more in-depth description of peptide synthesis is give below for a 27-component tripeptide combinatorial library prepared using standard solid-phase mix and split protocols.[33] This library, $X_1X_2X_3$, was prepared so that X_1 = R, K, or L; X_2 = F, S, or Y; and X_3 = D, E, or G. At the start of the synthesis, equal molar quantities of the preloaded Wang resins *N*-α-Fmoc-L-aspartic acid γ-*tert*-butyl ester, N-α-Fmoc-L-glutamic acid γ-*tert*-butyl ester, and N-α-Fmoc-glycine (the C-terminal residues) were mixed in a nitrogen-agitated reaction vessel with dimethylformamide (DMF) prior to the removal of the N-terminal Fmoc protecting group with 20% piperidine in DMF. The resulting resin mixture was split into three equal portions and placed into separate reaction vessels for the addition of the next amino acid residues. Amino acid coupling reactions were performed by the addition of preactivated benzotriazol-1-yloxy (OBt) esters of each amino acid being added to the Fmoc-deprotected resin. Activated amino acid OBt esters were generated by reaction of the Fmoc amino acids (4.0 equiv) with 2-(1-*H*-benzotriazol-1-yl)-1,1,3,3-tetramethyluronium hexafluorophosphate (3.9 equiv), and 0.4 M *N*-methylmorpholine in DMF (4 equiv) to the reaction vessel containing the resin. After coupling the final N-terminal amino acid residues, the Fmoc protecting group was removed from the N-terminus of the peptide. The library was then cleaved from the solid-phase support and side-chain protecting groups were removed using a trifluoroacetic acid/phenol/water/thioanisole/ethanedithiol solution (82.5:5:5:5:2.5 by volume). The resin was filtered from the solution, and the peptides were precipitated using ether. The precipitates were washed several

(18) Julian, R. R.; Beauchamp, J. L. *Int. J. Mass Spectrom.* **2001**, *210*, 613−623. Julian, R. R.; Beauchamp, J. L. *J. Am. Soc. Mass Spectrom.* **2002**, *13*, 493−498. Julian, R. R.; Akin. M.; May, J. A.; Stoltz, B. M.; Beauchamp, J. L. *Int. J. Mass Spectrom.* **2002**, *220*, 87−96. Julian, R. R.; Beauchamp, J. L. *J. Am. Soc. Mass Spectrom.* **2004**, *15*, 616−624.
(19) For example see: Schalley, C. A. *Mass Spectrom. Rev.* **2001**, *20*, 253−309, and references therein.
(20) Tao, W. A.; Wu, L. M.; Cooks, R. G. *J. Am. Soc. Mass Spectrom.* **2001**, *12*, 490−496. Wu, L. M.; Meurer, E. C.; Young, B.; Yang, P. X.; Eberlin, M. N.; Cooks, R. G. *Int. J. Mass Spectrom.* **2004**, *231*, 103−111.
(21) Garcia, B.; Ramirez, J.; Wong, S.; Lebrilla, C. B. *Int. J. Mass Spectrom.* **2001**, *210*, 215−222. Ahn, S.; Cong, X.; Lebrilla, C. B. *J. Am. Soc. Mass Spectrom.* **2005**, *16*, 166−175.
(22) Lee, S.; Wyttenbach, T.; von Helden, G.; Bowers, M. T. *J. Am. Chem. Soc.* **1995**, *117*, 10159−10160.
(23) Rudiger, V.; Schneider, H. J.; Solov'ev, V. P.; Kazachenko, V. P.; Raevsky, O. A. *Eur. J. Org. Chem.* **1943**, *8*, 1847−1856.
(24) Crowe, M. C.; Brodbelt, J. S. *J. Am. Soc. Mass Spectrom.* **2003**, *14*, 1148−1157. Sherman, C. L.; Brodbelt, J. S. *Anal. Chem.* **2003**, *75*, 1828−1836.
(25) Colgrave M. L.; Bramwell, C. J.; Creaser, C. S. *Int. J. Mass Spectrom.* **2003**, *229*, 209−216.
(26) Tao W. A.; Zhang, D. X.; Wang, F.; Thomas, P. D.; Cooks, R. G. *Anal. Chem.* **1999**, *71*, 4427−4429. Zhang, D. X.; Tao, W. A.; Cooks, R. G. *Int. J. Mass Spectrom.* **2001**, *204*, 159−169.
(27) Ramirez, J.; Ahn, S. H.; Grigorean, G.; Lebrilla, C. B. *J. Am. Chem. Soc.* **2000**, *122*, 6884−6890.
(28) See, for example: Speranza, M. *Int. J. Mass Spectrom.* **2004**, *232*, 277−317, and references therein.
(29) Chu, I.-H.; Zhang, H.; Dearden, D. V. *J. Am. Chem. Soc.* **1993**, *115*, 5736−5744.
(30) More, M. B.; Ray, D.; Armentrout, P. B. *J. Am. Chem. Soc.* **1999**, *121*, 417−423.
(31) Brodbelt, J. S. *Int. J. Mass Spectrom.* **2000**, *200*, 57−69.
(32) Merrifield, R. B. *J. Am. Chem. Soc.* **1963**, *85*, 2149−2153. Carpino L. A.; Han, G. Y. *J. Org. Chem.* **1972**, *37*, 3404−3409. Wellings, D. A.; Atherton, E. *Methods Enzymol.* **1997**, *289*, 44−67.
(33) Lebl, M.; Krchnak, V. *Methods Enzymol.* **1997**, *289*, 336−392.

times with ether, dried, dissolved in an aqueous solution (30% acetic acid), and lyophilized. The following Wang resins were used for the synthesis of the peptides used in these experiments: *N*-α-Fmoc-L-aspartic acid *γ-tert*-butyl ester, *N*-α-Fmoc-L-glutamic acid *γ-tert*-butyl ester, *N*-α-Fmoc-glycine, *N*-α-Fmoc-L-alanine, *N*-α-Fmoc-L-valine, and *N*-α-Fmoc-*N*-*β*-triyl-L-asparagine. The following protected amino acid residues (Novabiochem) were used for the synthesis of the peptides used in these experiments: *N*-α-Fmoc-L-phenylalanine, *N*-α-Fmoc-*O-tert*-butyl-L-serine, *N*-α-Fmoc-*O-tert*-butyl-L-tyrosine, *N*-α-Fmoc-N^G-2,2,5,7,8-pentamethylchroman-6-sulfonyl-L-arginine, *N*-α-Fmoc-L-leucine, and N-α-Fmoc-*N*-*ϵ-tert*-Boc-L-lysine.

Electrospray Solutions. The mole ratio of peptide/crown ether required to fully complex the peptide to a prominent form was explored and was determined to be ~1:50. All samples were electrosprayed from solutions of water/acetonitrile/acetic acid (49:49:2). The dipeptide isobars were prepared in solutions containing 0.5 mM peptide with and without each of the following crown ethers (25 mM): 12C4 (98%, Aldrich); 15C5 (98%, Aldrich); 18C6 (99%, Aldrich); and, DB30C10 (98%, Aldrich). A mixture of the three dipeptides (0.5 mM total, 0.167 mM each dipeptide) was prepared with and without each of the crown ethers (25 mM). The 27-component library (0.5 mM, 384.2 average molecular weight) was prepared with and without 18C6 (25 mM).

IMS−MS Analysis. In these experiments, two IMS−MS instruments were used to analyze peptide−crown complexes: (1) a high-resolution IMS−MS instrument[9,34] and (2) a lower resolution instrument that incorporates collision-induced dissociation (CID) prior to mass analysis (IMS-CID-MS).[35−38] These instruments have been described in detail previously, and only a brief overview of IMS will be given here.

Samples are electrosprayed into the source of an IMS−MS instrument. The electrosprayed ions are guided into the front of the instrument, and a short (~100 μs) pulse of ions is allowed into the drift tube. These ions traverse through a drift tube filled with helium buffer gas, under the influence of a uniform electric field. Ions are separated from one another based on the number of collisions with the helium buffer gas and by the drift force that is imparted on them by the electric field. In general, highly charged ions experience a greater drift force and therefore have higher mobilities than ions of the same m/z that have a lower charge state. Ions that are larger/more elongated experience more collisions with the buffer gas and have lower mobilities than those that are more compact.[39,40] Once an ion reaches the end of the drift tube, it is pulsed orthogonally into a reflectron time-of-flight MS (TOFMS) where flight time distributions are recorded. A standard multipoint calibration converts flight times to mass-to-charge ratios. This means that a drift time and a flight time are measured for each ion that enters the instrument. We refer to this as a nested approach.[41]

The IMS-CID-MS instrument is equipped with a split field region[37] at the back of the drift tube as well as an octopole collision cell[35] after the drift tube. These features were incorporated so that ions can be fragmented after they traverse through the drift region of the instrument in a parallel fashion.[35] For experiments where we want to generate peptide fragments, we increase the field at the back of the drift tube and/or add argon gas (0.1 mTorr) to the octopole collision cell. For experiments where precursor ions are desired, the field at the back of the drift tube was lowered and the argon collision gas was removed from the collision cell, using the octopole as an ion guide. Upon exiting the collision cell, ions enter the source region of a reflectron geometry TOFMS where high-frequency, high-voltage potentials were used to initiate measurements of flight times (and hence m/z ratios).

Determination of Cross Sections. Once the drift time and m/z for an ion are determined a collision cross section can be determined using the following equation,[11]

$$\Omega = \frac{(18\pi)^{1/2}}{16}\frac{ze}{(k_bT)^{1/2}}\left[\frac{1}{m_I}+\frac{1}{m_B}\right]^{1/2}\frac{t_D E}{L}\frac{760}{P}\frac{T}{273.2}\frac{1}{N}$$

where t_D corresponds to the drift time, and E, L, P, and T correspond to the electric field strength, drift tube length, and buffer gas pressure and temperature, respectively; m_I and m_B correspond to the masses of the ion and buffer gas, respectively. The other terms, ze, k_b, and N, correspond to the charge on the ion, Boltzmann's constant, and neutral number density, respectively. The calculation of a cross section takes into account pressure, temperature, and other instrumental parameters and therefore allows for the comparison of an ion from instrument to instrument and from experiment to experiment.

RESULTS AND DISCUSSION

IMS−MS Analysis of the Isobaric Dipeptides RA, KV, and LN. The peptides RA, KV, and LN have calculated monoisotopic masses of 245.1487, 245.1739, and 245.1375 Da, respectively (a range of 0.036 Da). The mass resolution required to separate RA and LN is on the order of 20 000. Although this resolution could be obtained in a high-resolution mass spectrometer, such as an ion cyclotron resonance instrument, we use these peptides to demonstrate the chemistry involved between crown ethers and peptides containing basic and nonbasic residues. The three peptides were analyzed individually, as well as in a mixture by high-resolution IMS−MS, in order to determine whether the naked peptide ions could be separated using IMS. Figure 2 shows the four, two-dimensional t_D (m/z) data sets that were obtained. These peptides form predominately $[M + H]^+$ ions. We also

(34) Counterman, A. E.; Valentine, S. J.; Srebalus, C. A.; Henderson, S. C.; Hoaglund, C. S.; Clemmer, D. E. *J. Am. Soc. Mass Spectrom.* **1998**, *9*, 743−759.

(35) Hoaglund-Hyzer, C. S.; Li, J.; Clemmer, D. E. *Anal. Chem.* **2000**, *72*, 2737−2740.

(36) Hoaglund-Hyzer, C. S.; Clemmer, D. E. *Anal. Chem.* **2001**, *73*, 177−184.

(37) Valentine, S. J.; Koeniger, S. L.; Clemmer, D. E. *Anal. Chem.* **2003**, *75*, 6202−6208.

(38) Koeniger, S. L.; Valentine, S. J.; Myung, S.; Plasencia, M.; Lee, Y. L.; Clemmer, D. E. *J. Proteome Res.* **2005**, *4*, 25−35.

(39) For reviews of ion mobility studies, see: Hagen, D. F. *Anal. Chem.* **1979**, *51*, 870−874. St. Louis, R. H.; Hill, H. H. *Crit. Rev. Anal. Chem.* **1990**, *21*, 321−355. von Helden, G.; Hsu, M. T.; Kemper, P. R.; Bowers, M. T. *J. Chem. Phys.* **1991**, *95*, 3835−3837. Jarrold, M. F. *J. Phys. Chem.* **1995**, *99*, 11−21. Clemmer, D. E.; Jarrold, M. F. *J. Mass Spectrom.* **1997**, *32*, 577−592. Liu, Y.; Valentine, S. J.; Counterman, A. E.; Hoaglund, C. S.; Clemmer, D. E. *Anal. Chem.* **1997**, *69*, 728A−735A.

(40) Chen, Y. L.; Collings, B. A.; Douglas, D. J. *J. Am. Soc. Mass Spectrom.* **1997**, *8*, 681−687.

(41) Hoaglund, C. S.; Valentine, S. J.; Sporleder, C. R.; Reilly, J. P.; Clemmer, D. E. *Anal. Chem.* **1998**, *70*, 2236−2242.

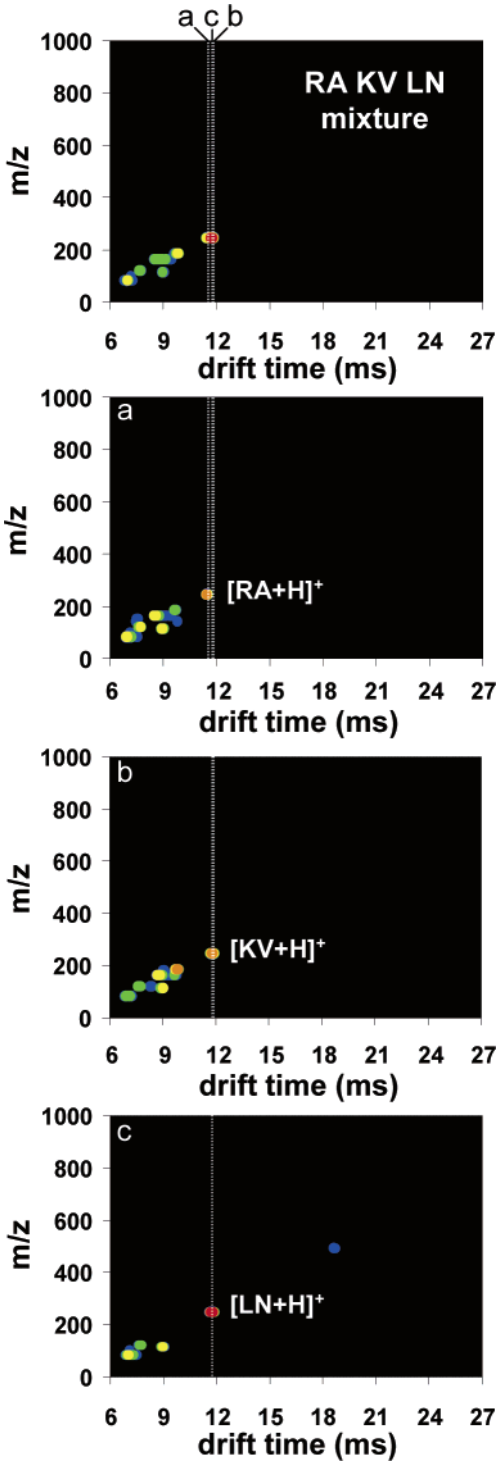

Figure 2. Two dimensional plots of drift times (ms) versus *m*/*z* ratios obtained from an ESI IMS-TOF experiment for the mixture (RA, KV, LN), (a) RA, (b) KV, and (c) LN peptides. The intensity of different features is shown using a false color scheme in which the least intense features are represented in blue and the most intense features are represented in red. The $[M + H]^+$ ion for each peptide is indicated with a white line within the 2D plots, (a) RA, (b) KV, and (c) LN.

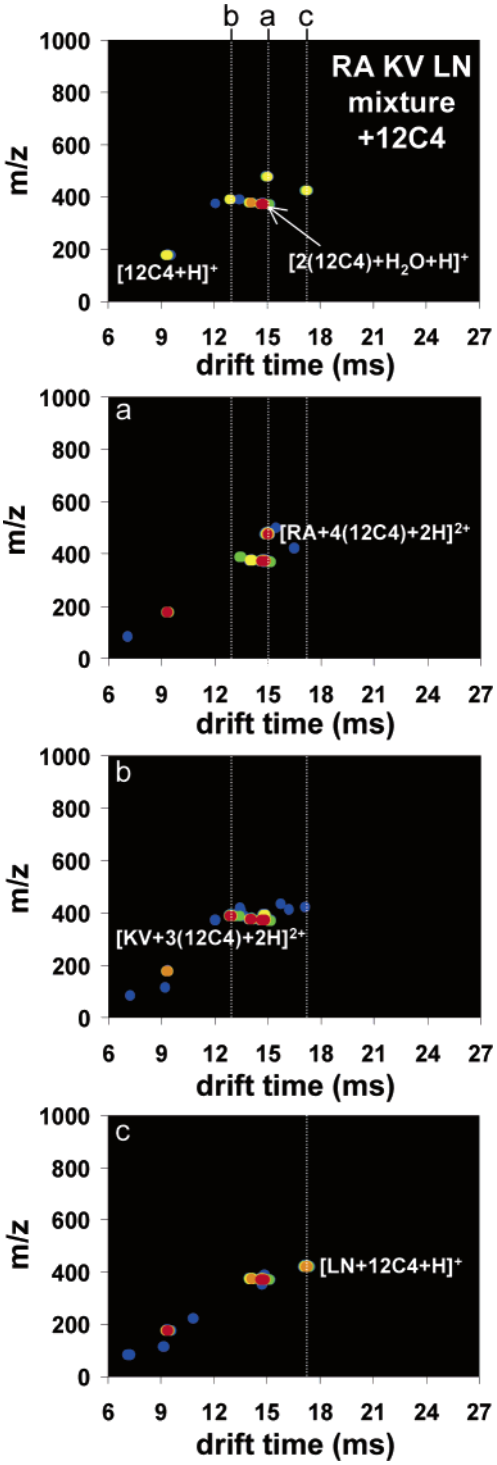

Figure 3. Two dimensional plots of drift times (ms) versus *m*/*z* ratios as shown in Figure 2 with the incorporation of 12C4 in each sample. The intensity of different features is shown using a false color scheme in which the least intense features are represented in blue and the most intense features are represented in red. The peptide−12C4 complexes are indicated by a white line within the 2D plot. Peptides are resolved into the following complexes indicated by white lines within the 2D plot: (a) $[RA + 4(12C4) + 2H]^+$, (b) $[KV + 3(12C4) + 2H]^+$, and (c) $[LN + 12C4 + H]^+$.

observe some $[M + 2H]^{2+}$ ions for the RA and KV peptides. Individual analyses were compared with the data set for the mixture to make assignments. The $[RA + H]^+$ ion, having a drift time of 11.5 ms, can be slightly resolved from the other two peptide ions $[KV + H]^+$ and $[LN + H]^+$, which have indistinguishable mobilities in the mixture, both having a drift time of 11.8 ms. We note the presence of some peaks at low *m*/*z*; these can be ascribed to a range of species including some multiply charged ions as well as byproducts of the synthesis. The enhanced

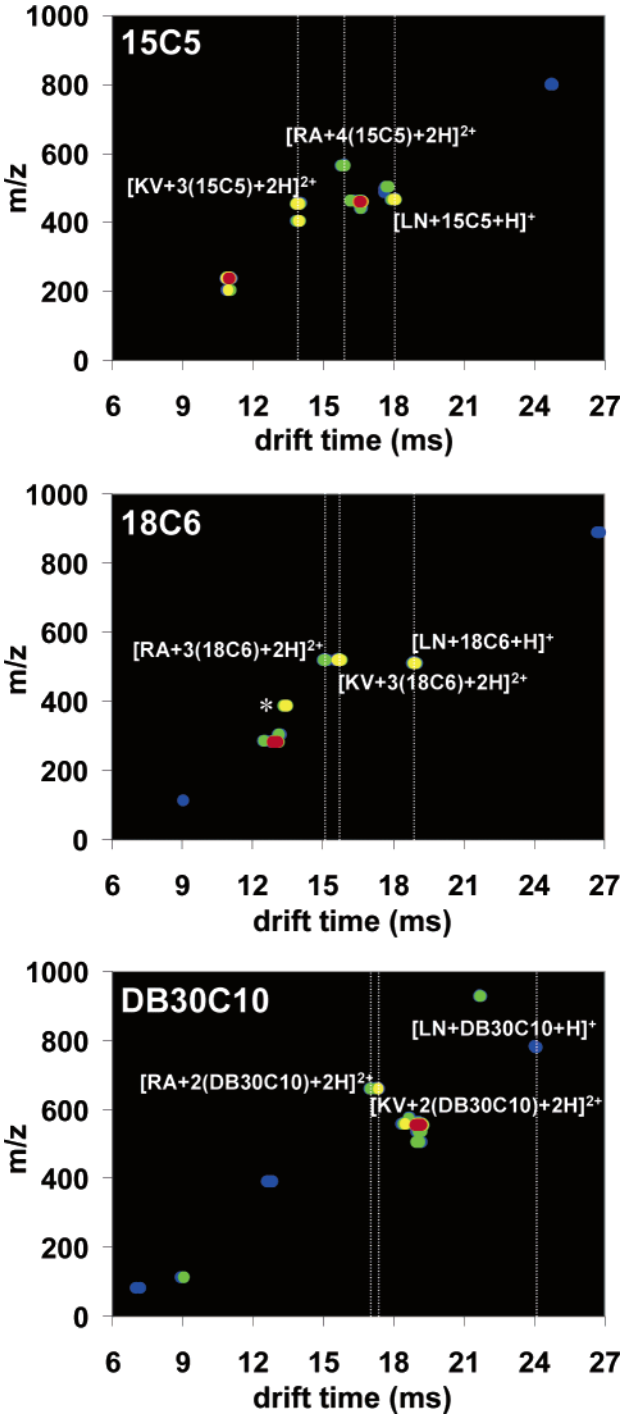

Figure 4. Two dimensional plots of drift times (ms) versus *m/z* ratios for the complexes formed when 15C5, 18C6, and DB30C10 are added to a mixture consisting of RA, KV, and LN. Each resolvable peptide−crown ether complex peak is indicated with white lines within the 2D plot. As shown in each spectrum, LN peptide only complexes with one crown because it lacks basic amino acids; therefore, the crown can only complex with the N-terminus of the peptide. The data indicate that as the size of the crown ether increases fewer crowns complex with peptides containing basic lysine and arginine residues. The irresolvable peaks $[RA + 2(18C6) + 2H]^+$ and $[KV + 2(18C6) + 2H]^+$ are indicated by an asterisk in the 18C6 spectrum.

ionization efficiency that arises upon addition of crowns reduces the relative abundances of these ions.

IMS−MS Analysis of Dipeptide−Crown Complexes. Figures 3 and 4 show typical data sets obtained upon addition of each

Table 1. Cross Sections for Non-Peptide−Crown Ether Complexes Formed from ESI Peptide/Crown Mixtures

crown ether complex	m/z[a]	t_D (ms)	Ω (Å^2)
$[12C4+H]^+$	177.1	9.3	75
$[2(12C4) + H]^+$	353.2	14.7	119
$[2(12C4) + H_2O + H]^+$	371.2	14.8	119
$[2(12C4) + Na]^+$	375.2	14.1	114
$[2(12C4) + K]^+$	391.3	14.9	120
$[15C5 + H_2O+H]^+$	239.1	11.2	90
$[2(15C5) + H]^+$	441.3	16.8	137
$[2(15C5) + H_2O + H]^+$	459.3	16.8	136
$[2(15C5) + Na]^+$	463.3	16.4	133
$[2(15C5) + K]^+$	479.4	16.5	134
$[18C6 + H_2O + H]^+$	283.2	13.2	106
$[18C6 + Na]^+$	287.1	12.7	102
$[18C6 + K]^+$	303.3	13.3	108
$[DB30C10 + H]^+$	537.3	19.2	155
$[DB30C10 + H_2O + H]^+$	555.3	19.1	154
$[DB30C10 + Na]^+$	559.3	18.5	150
$[DB30C10 + K]^+$	575.4	18.6	151

[a] Calculated m/z values from monoisotopic masses.

of the crown ethers to the peptide solutions. We observe a number of peptide−crown complexes, as well as the following: protonated crown ether monomers and clusters; crowns complexed with H_3O^+; and crowns complexed with Na^+ and K^+ impurities. The m/z values, drift times, and cross sections (as calculated from eq 1) of all of the assigned clusters and adducts are given in Tables 1 and 2.

It is worthwhile to examine some systems in more detail. Figure 3 shows IMS−MS data sets for the three individual peptides sprayed with 12C4 as well as the mixture of peptides with 12C4. There are three dominant features that are assigned to peptide−crown complexes, as well as peaks that correspond to 12C4 without peptides, existing as $[2(12C4) + H_2O + H]^+$ and $[12C4 + H]^+$. The RA peptide forms primarily the $[RA + 4(12C4) + 2H]^{2+}$ ion having a drift time of 15.0 ms. In this case, addition of the 12C4 results in an increase in the charge state of the complex (+2) relative to the peptide with no crown added. This is often the case for these systems and has been reported previously for complexes of tetralysine with 18C6.[18] The KV peptide forms primarily $[KV + 3(12C4) + 2H]^{2+}$ having a drift time of 12.9 ms. The LN peptide, containing no basic amino acids, adds a single 12C4 molecule to the charged N-termius to form the $[LN + 12C4 + H]^+$ complex having a drift time of 17.3 ms. The new drift times, 12.9, 15.0, and 17.3 ms, allow the KV, RA, and LN peptides to be easily resolved as complexes.

Figure 4 provides a comparable illustration of the data obtained from addition of each of the other crown ethers (15C5, 18C6, DB30C10) to the RA, KV, and LN mixture. As above, peak assignments for the mixtures were determined by running the peptides individually with each crown. Overall, the data show that complexes of 15C5 are similar to those formed with 12C4. The most intense features correspond to $[RA + 4(15C5) + 2H]^{2+}$, $[KV + 3(15C5) + 2H]^{2+}$, and $[LN + 15C5 + H]^+$. In this case, the dominant peaks are clearly separated as complexes. In the case of 18C6−peptide complexes, we observe that RA and KV favor $[M + 2(18C6) + 2H]^{2+}$, which have nearly identical drift times and m/z. Although these ions are not resolved as complexes, the

Table 2. Crown Ether Complexes with Peptide Isobars RA, KV, and LN

	peptide ion	peptide−12C4 complex	peptide−15C5 complex	peptide−18C6 complex	peptide−DB30C10 complex
RA	$[RA + H]^+$	$[RA + 4(12C4) + 2H]^{2+}$	$[RA + 4(15C5) + 2H]^{2+}$	$[RA + 3(18C6) + 2H]^{2+}$	$[RA + 2(DB30C10) + 2H]^{2+}$
m/z[a]	246.2	475.8	563.8	519.8	659.8
t_D (ms)	11.5	15.0	16.0	15.3	17.2
Ω (Å^2)	93	242	258	247	277
KV	$[KV + H]^+$	$[KV + 3(12C4) + 2H]^{2+}$	$[KV + 3(15C5) + 2H]^{2+}$	$[KV + 3(18C6) + 2H]^{2+}$	$[KV + 2(DB30C10) + 2H]^{2+}$
m/z[a]	246.2	387.8	453.8	519.8	659.9
t_D (ms)	11.8	12.9	14.1	15.9	17.5
Ω (Å^2)	96	208	227	256	282
LN	$[LN + H]^+$	$[LN + 12C4 + H]^+$	$[LN + 15C5 + H]^+$	$[LN + 18C6 + H]^+$	$[LN + DB30C10 + H]^+$
m/z[a]	246.1	422.3	466.3	510.3	782.4
t_D (ms)	11.8	17.3	18.2	19.1	24.3
Ω (Å^2)	95	140	148	155	197

[a] Calculated m/z values from monoisotopic masses.

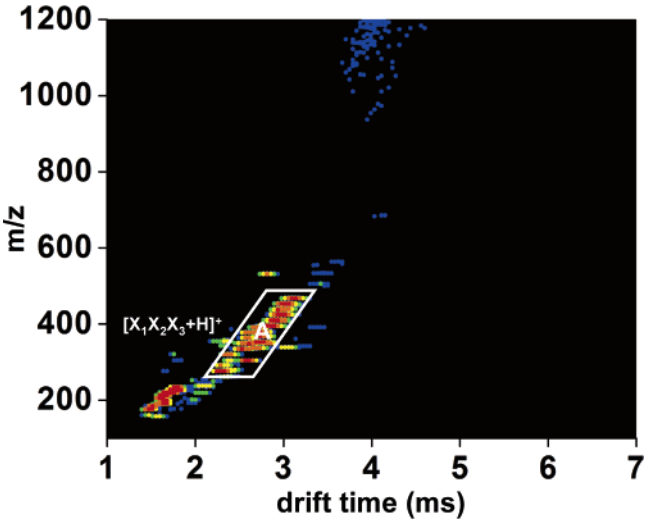

Figure 5. Two dimensional plots of drift times (ms) versus m/z ratios for the $X_1X_2X_3$, 27-component tripeptide library, where X_1 = R, K or L, X_2 = F, S or Y, and X_3 = D, E or G. The most intense peaks correspond to $[X_1X_2X_3 + H]^+$ ion and are indicated by a white parallelogram (A) within the 2D plot. These ions are observed within the m/z values of 276.2−467.2 and drift times of 2.2−3.3 ms.

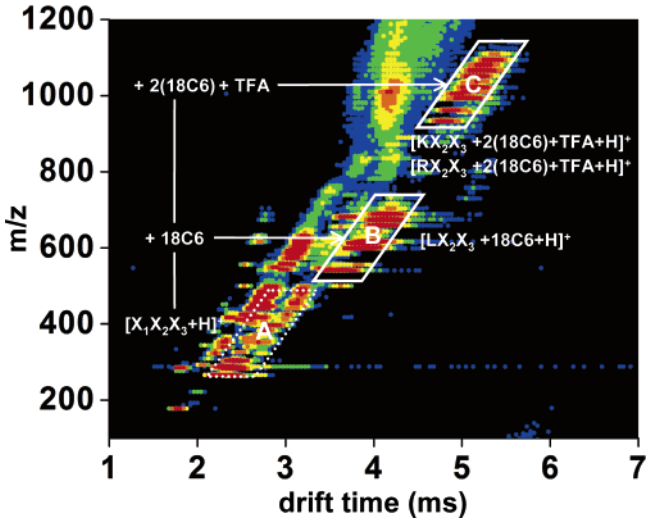

Figure 6. Two dimensional plots of drift times (ms) versus m/z ratios of peptides shown in Figure 5 with the incorporation of 18C6 into the mixture. The library peptides are separated into two distinct regions in the spectrum: (B) The nine LX_2X_3 library peptides complexed to a single 18C6 molecule in their N-terminus thereby creating $[LX_2X_3 + 18C6 + H]^+$ ions (m/z 540.3−688.4 and drift times of 3.4−4.4 ms). (C) The 18 basic peptides containing residues RX_2X_3 and KX_2X_3 complexed with two 18C6 molecules and a TFA molecule to create $[RX_2X_3 + 2(18C6) + TFA + H]^+$ and $[KX_2X_3 + 2(18C6) + TFA + H]^+$ ion (m/z 933.5−1109.5 and drift times of 4.6−5.6 ms).

less abundant $[RA + 3(18C6) + 2H]^{2+}$ and $[KV + 3(18C6) + 2H]^{2+}$ forms (having drift times of 15.3 and 15.9 ms, respectively) are separated. The LN peptide favors the $[LN + 18C6 + H]^+$ complex and has a drift time of 19.1 ms. This peak is easily resolved from the others. Finally, we note that addition of DB30C10 favors the $[RA + 2(DB30C10) + 2H]^{2+}$ and $[KV + 2(DB30C10) + 2H]^{2+}$ complexes with drift times of 17.2 and 17.9 ms, respectively. LN forms $[LN + DB30C10 + H]^+$ with a drift time of 24.3 ms.

Overall, these data show that by carefully selecting a complexing agent it is possible to resolve peptides that have identical mobilities; additionally, the resulting positions of peaks vary depending upon the number of agents that complex to the peptide as well as the resulting charge state.

Complexes of 18C6 with a Tripeptide Library. The studies of the three dipeptides with the series of crowns encouraged us to extend these ideas to a larger mixture of 27 tripeptides (described above). Here, we limit the study to peptide complexes with 18C6. Additionally, these experiments are carried out on our low-resolution IMS−MS instrument that is equipped with a high-field region at the back of the drift tube and a collision cell to enable fragmentation of molecular ions and complexes after the drift region and prior to the time of flight.[37] As noted above, the peptide mixture contains 27 sequences having the form $X_1X_2X_3$, where X_1 is R, K or L, X_2 is F, S, or Y, and X_3 is D, E or G. Each peptide has a unique mass.

Figure 5 shows the IMS−MS data set that is recorded for analysis of the library with no added 18C6. The distribution from 2.2 to 3.2 ms (and m/z = 276.2−467.2) corresponds to singly charged $[X_1X_2X_3 + H]^+$ ions; additionally, a lower abundance series of peaks (from ~1.5 to 2.0 ms) corresponds to formation

Table 3. Assignment for Library Peptide−18C6 Complexes

no.[a]	$X_1X_2X_3$[b]	$[X_1X_2X_3 + H]^+$[c]	$[X_1X_2X_3 + 18C6 + H]^+$[d]	$[X_1X_2X_3 + 2(18C6) + TFA + H]^+$[e]
1	LSG	276.2 (276.2)	540.4 (540.3)	
2	KSG	291.2 (291.2)		933.3 (933.5)
3	RSG	319.3 (319.2)		961.3 (961.5)
4	LSD	334.2 (334.2)	598.4 (598.3)	
5	LFG	336.3 (336.2)	600.3 (600.3)	
6	LSE	348.1 (348.2)	612.3 (612.3)	
7	KSD	349.2 (349.2)		991.2 (991.5)
8	KFG	351.2 (351.2)		993.3 (993.5)
9	LYG	352.3 (352.2)	616.4 (616.3)	
10	KSE	363.3 (363.2)		1005.1 (1005.5)
11	KYG	367.2 (367.2)		1009.4 (1009.5)
12	RSD	377.1 (377.2)		1019.5 (1019.5)
13	RFG	379.2 (379.2)		1021.3 (1021.5)
14	RSE	391.2 (391.2)		1033.3 (1033.5)
15	LFD	394.2 (394.2)	658.2 (658.4)	
16	RYG	395.2 (395.2)		1037.3 (1037.5)
17	LFE	408.3 (408.2)	672.3 (672.4)	
18	KFD	409.2 (409.2)		1051.2 (1051.5)
19	LYD	410.2 (410.2)	674.3 (674.4)	
20	KFE	423.3 (423.2)		1065.5 (1065.5)
21	LYE	424.3 (424.2)	688.3 (688.4)	
22	KYD	425.3 (425.2)		1067.1 (1067.5)
23	RFD	437.2 (437.2)		1079.3 (1079.5)
24	KYE	439.2 (439.2)		1081.2 (1081.5)
25	RFE	451.1 (451.2)		1093.2 (1093.5)
26	RYD	453.2 (453.2)		1095.1 (1095.5)
27	RYE	467.1 (467.2)		1109.4 (1109.5)

[a] These numbers correspond to the sequences in the second column and are used in Figure 8 to identify peaks. [b] Sequence of the three-residue library peptides. In this library, the X_1 is varied over the amino acids R, K and L; X_2 over F, S and Y; and X_3 over D, E and G. [c] Monoisotopic m/z of the peaks observed for the plus one monomer of the three residue peptides, calculated m/z values in parentheses [d] Monoisotopic m/z of the peaks observed for the complexation of a single 18C6 to the plus one monomer of the peptide, calculated m/z values in parentheses. This type of complexation was only seen for the LX_2X_3 peptides. [e] Monoisotopic m/z of peaks observed for the complexation of two 18C6 and a single TFA molecule to a monomer of the peptide (creating a plus one complex) calculated m/z values in parentheses. This type of complexation was only seen for the RX_2X_3 and KX_2X_3 peptides.

of some doubly protonated ions. We have outlined singly charged family of ions (as a bold white line) as a visual guide.

Figure 6 shows the distribution that is obtained when 18C6 is added to the mixture. The most striking feature of these data is that the peaks associated with the naked peptide ions decrease in relative intensity and several new families of peaks can be observed. The observation of multiple families indicates that there is a variation in the 18C6−peptide binding interactions that is sequence dependent. For simplicity, we focus our discussion on regions of the data set that are assigned to expected peptide−18C6 complexes. There is clearly evidence of other multimer formation centered at ~2.2, 2.7, 3.2, and 4.2 ms and m/z ~300, 450, 600, and 1000, respectively. Although a number of these peaks are assignable, there is no clear benefit in discussing these assignments here.

Figure 6 highlights two groups of peaks that are particularly interesting. The first group (having drift times of 3.2−4.7 ms) contains the nine peptides that can be assigned to the leucine-containing sequences, LX_2X_3 with a single 18C6 added. It is possible to assign all nine of the leucine sequences in this region. The second set of peptides (from 4.8 to 5.8 ms) contains the other

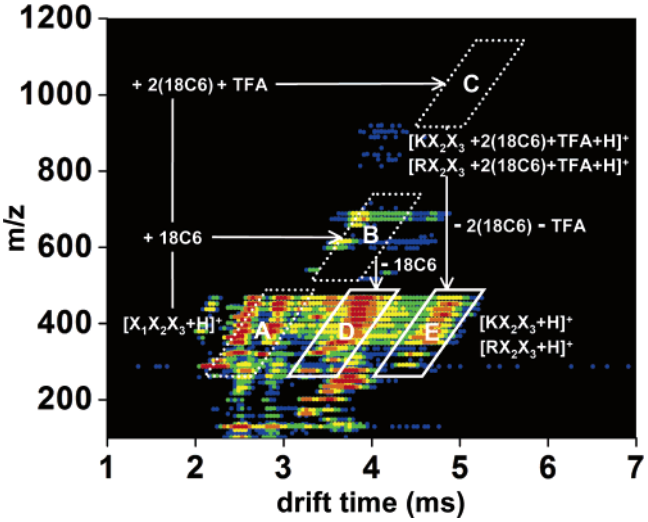

Figure 7. Two dimensional plots of drift times (ms) versus m/z ratios obtained by inducing fragmentation for the 18C6 incorporated $X_1X_2X_3$ library as shown in Figure 6. Shown in the spectrum is the cyclic step required to return to the original $[X_1X_2X_3 + H]^+$ ions as indicated by the arrows. Region D (m/z = 276.2−424.2 and drift times of 3.2−4.2 ms), represents the position of $[LX_2X_3 + H]^+$ peptides obtained by fragmenting $[LX_2X_3 + 18C6 + H]^+$ (B) ions. Region E (m/z = 291.2−467.2 and drift times of 4.2−5.2 ms) represents $[RX_2X_3 + H]^+$ and $[KX_2X_3 + H]^+$ ions obtained by fragmenting $[RX_2X_3 + 2(18C6) + TFA + H]^+$ and $[KX_2X_3 + 2(18C6) + TFA + H]^+$ (C) ions. Region A indicates the original location of the 27 $[X_1X_2X_3 + H]^+$ prior to addition of the 18C6 gas-phase stationary phase.

18 peptides from the library having basic amino acids in their X_1 position, RX_2X_3 and KX_2X_3. These 18 peptides add two 18C6 molecules and a trifluoroacetic acid (TFA) molecule. The TFA molecules are in the solution due to residual TFA from the cleavage reaction during the synthesis of the library. The masses for all of these ions labeled in Figures 5 and 6 are summarized in Table 3.

Figure 7 demonstrates the ability to remove all of the 18C6, making it possible to generate peptide ions (with no 18C6). This can be done immediately as the ions exit the drift tube (using the split field system described elsewhere) or in an octopole geometry collision cell (filled with 0.1 mTorr Ar) or by a combination of both. Inspection of these data shows that the $[X_1X_2X_3 + H]^+$ ions are generated from the complexes efficiently. The peptides are found at their original mass, and the RX_2X_3 and KX_2X_3 peptides are found significantly separated from the LX_2X_3 in the mobility dimension.

A clear advantage of this cycle is that new distributions have been resolved according to the number of basic sites within the peptides, which is dictated by the first residue of these peptides. One way to assess how well the basic ions were separated from the nonbasic ions (and to assign them) is to examine the difference between the original peptide distribution (with no added 18C6) and the separated distributions. Integration of the narrow range of peaks in Figure 5 over the drift time range 2.2−3.3 ms gives the spectrum containing peaks for all 27 components of the library. We have labeled these peaks 1−27, and the assignments can be made from the same numbering system, used in Table 3. A different mass spectrum is obtained by integrating the data in Figure 7 over a drift time range of 4.2−5.2 ms. The peaks are readily assigned to the 18 sequences containing a basic residue

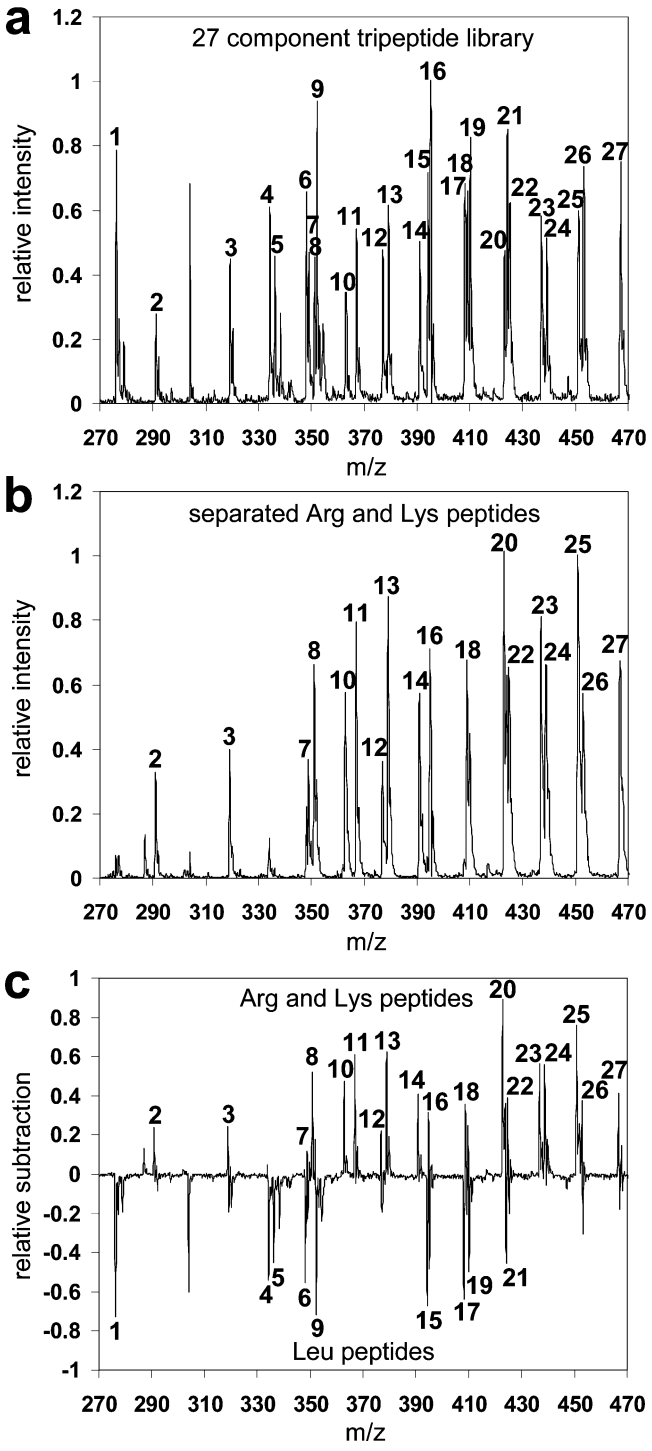

Figure 8. Normalized integrated *m*/*z* slices for (a) data from drift times 2.2−3.3 ms from the data for the 27-component library peptides with no 18C6 complexation (data plotted in Figure 5) and (b) from drift times 4.2−5.2 ms from the fragmentation of the 18C6 gas-phase stationary phase molecule from the separated basic peptide−18C6 complexes (data plotted in Figure 7). Subtraction of the integrated *m*/*z* spectrum (a) from the integrated *m*/*z* spectrum (b) results in the *m*/*z* subtraction spectrum shown in (c). This resulting spectrum indicates that the RX_2X_3 and KX_2X_3 peptides, having positive intensities, were separated from the LX_2X_3 peptides, having negative intensities. Peaks are labeled using the numbers indicated for sequences in Table 3.

in the X_1 position. Subtraction of these spectra shows that the missing peptides are the nine peptides that contain leucine in the first position, indicating that they were separated from the arginine- and lysine-containing peptides.

Considerations of Collision Cross Sections. As a final note, we briefly consider the collision cross sections for the different complexes associated with the separation of the three dipeptides and four different crowns. From the data in Tables 1 and 2, we note a number of interesting trends. The present system was designed to maximize the impact of the adduct formation on the cross section. That is, the cross sections for the ligands that were chosen range from 75 Å^2 for 12C4 to 155 Å^2 for DB30C10, values that are near the cross sections for the isolated dipeptides, 93, 96, and 95 Å^2 for the singly protonated RA, KV, and LN sequences, respectively. From this consideration, one anticipates that addition of these ligands will have a significant impact on the separation. This effect is observed experimentally. However, we note that the choice of these ligands may also influence the ion charge state; crown ether binding appears to sequester protons and leads to complexes that may have higher charge states. Thus, the decrease in mobility that is anticipated purely from the increase in size, associated with the addition of a bulky ligand, may be mitigated by the increase in mobility associated with a higher charge state.

From Figures 3 and 4, we can observe these effects. Addition of each 12C4, 15C5, 18C6, and DB30C10 to the LN peptide results in the formation of singly protonated 1:1 complexes having drift times (and cross sections) of 17.3 (140 Å^2), 18.2 (148 Å^2), 19.1 (155 Å^2), and 24.3 (197 Å^2) ms, respectively—values that systematically increase with the size of the ligand. In contrast, although the complex of RA with four 15C5 ligands has a much larger cross section, 258 Å^2, it also carries twice the charge (and thus, experiences a greater drift force) leading to a substantially shorter drift time, 16 ms. Overall, we point this out because it emphasizes the need to judiciously choose a shift reagent when using this approach to resolve different species. Finally, as this work is extended to larger peptides, we expect smaller relative shifts in cross sections upon addition of the same number of ligands. In such cases, if many charges are sequestered, complexes may have higher mobilites than the naked ions. There may be the need to develop larger molecules for addition to larger systems in order to significantly influence the separation of larger peptides.

SUMMARY AND CONCLUSIONS

This work has examined the use of a series of crown ethers as shift reagents for peptide analysis by ion mobility spectrometry. The method that has been developed involves adding an excess of crown ether to a mixture of peptides. The complexes that are formed depend on the chemical properties of the peptide, and thus, it is possible to shift the mobilities of components having similar masses or cross sections but different chemical compositions. This was demonstrated for a series of dipeptides as well as a library of 27 tripeptides; in the latter case, peptides containing leucine are shifted with respect to those containing arginine or lysine and can be readily distinguished based on the mobility shift. Once the peptide complexes are separated, it is possible to use collisional activation to generate the naked peptide ions for MS analysis. Cross sections for the complexes that were observed were reported.

A significant concern in the development of this method is that the addition of the crown to the peptide mixture may dramatically increase the complexity of the system. For components that cannot

be separated otherwise, the increase in complexity may be an acceptable tradeoff. As noted by others, there appears to be a significant increase in the ionization efficiency of peptide/crown complexes (compared with peptides alone).[18] This advantage arises because the crown−peptide complex sequesters the proton during the ESI process. Thus, while the system becomes more complex, the signals of individual components actually increase in the presence of the crown. We are currently extending the approach to more complicated mixtures of larger peptides generated by enzymatic digestion of proteins (and protein mixtures).[42]

(42) Bohrer, B.; Merenbloom, S. I.; Koeniger, S. L.; Hilderbrand, A. E.; Clemmer, D. E., work in progress.

ACKNOWLEDGMENT

This work was funded in part by grants from the National Institutes of Health (AG024547 and GM59145) and the National Science Foundation (CHE-0078737). Additional support is from the Indiana University METACyt initiative funded by the Lilly Endowment. We are grateful for many stimulating discussions with Dr. Ryan Julian.

Received for review March 9, 2006. Accepted July 19, 2006.

AC060439V